BOL/QMW/M/0017.1

Outstanding Design Issues and Actions Arising

1) The effect of diffraction at the input slit needs to be more fully evaluat (WDD report by 13/6/97)

2) ASAP and straylight analysis of photometer should proceed using EA's design and any updates to same (TR and Martin Caldwell - report by 13/6/97)

Matt also suggests that the straylight folk should contact Albrecht Poglitsch to see what's been done for the PHOC.

3) Can the concave grating be manufactured and with what RMS error (KD to contact Hyperfine)

4) What is performance of the concave grating on IRTS/FILM built by Hitachi (BMS to contact Takao Nakagawa - report by 13/6/97)

5) What manufacturers are available for the difficult aspheric optics (KD, BM - report by 13/6/97)

6) Contact Petit at University of Marseille re grating efficiency code (KD report by 13/6/97)

7) What alignment tolerances are required for the various spectrometer design (KD, EA - report by 13/6/97)

8) What size are the camera mirrors in the planar grating design? (EA - repo by 13/6/97)

9) Outline design for a cross disperser system to include in the spectrometerdesigns (BMS by 30/5/97 for EA and KD to include in designs by 13/6/97)

10) Investigate design of piezo-electric grating drive (IH report by 13/6/97)

11) What is the overall alignment budget betwen the BOL instrument and the FIRST satellite. (EA report by 13/6/97)

12) An end-to-end performance model is required - this partially exists in MathCad (yuek!) (MJG, WKPG and BMS to combine efforts and report on progress 13/6/97). As part of this exercise an estimate of total filter throughput fo both channels is required (PARA report by 13/6/97)

(and Matt says "CHANGE YEUK TO YIPEEE" - hmmmmm!)

Inputs to the IID

Matt presented the inputs required for IID and the following actions were noted:

1) A quick update is required for week beginning 12/5/97 - (BM and MJG).

2) Detailed revisions of the cryo-harness definition, mass estimates and thermal loads are required for 4/6/97, when a preliminary IID meeting will be held at ESTEC (MJG, BM, AGM, PRH, CRC). CRC will coordinate, with AGM = point of contact at QMW.

3) Realistic data rates are required for the 4/6/97 meeting (MJG, WKG, CRC, KJK). KJK to coordinate.

4) The top level description needs to be completely revised (MJG, BMS) New version to be done before 4/6/97.

Dear All,

Summary and Actions of BOL Grating Working Group Meeting of 9-MAY-1997

Prepared by: B.M. Swinyard - RAL 12-MAY-1997

Attendence and Contact Details:

Sye Murray	QMW	0171-975-5010	a.g.murray@qmw.ac.uk
Bruno Maffei	QMW	0171-975-4039	b.maffei@qmw.ac.uk
Peter Ade	QMW	0171-975-5032	p.a.r.ade@qmw.ac.uk
Ian Hepburn	MSSL	01483 204101	IDH@mssl.ucl.ac.uk
Peter Hastings	ROE	0131 668 8226	prh@roe.ac.uk
		fax 0131 668 1130	
William Duncan	OI	01865 882855	wlliam.duncan@oxinst.co.uk
		fax 01865 881567	
Kjetil Dohlen	OM	+33 495 044124	
		fax+33 491 621190	
Eli Etad	ROE	0131 668 8202	ea@roe.ac.uk
Colin Cunningham	ROE	0131 668 8223	crc@roe.ac.uk
Matt (mad dog)	Griffin	0171 975 5068	m.j.griffin@qmw.ac.uk
Tony Richards	RAL	01235 446146	a.r.richards@ral.ac.uk
Bruce Swinyard	RAL	01235 446405	b.m.swinyard@rl.ac.uk
		fax 01235 446667	

Summary of meeting:

1) The photometer ray trace design can be "frozen" to the one presented by El Etad. This uses f/9.6 input beam and should be updated to f/7.4 and 3.5m telescope with FOV 5.2 arcmin. Never-the-less straylight studies and diffraction limited analysis can proceed with the current design.

2) Two spectrometer designs have been presented that look to be reasonable a (probably!) can be built. One is the quasi Littrow mount with palanar garing and Gregorian camera to image the spectrum (EA); the other is a concave grati with a complex aspheric mirror to image the spectrum (KD). Both have questions about them that must be resolved before the next meeting.

The "pure" Rowland Circle option with a corrective field mirror looks increasingly difficult to implement.

3) A cross disperser offers some advantages (a large multiplex advantage) at the cost of some optical and straylight complexity. Further design studies a required.

4) A resolving power of 500 is theoretically achievable in a spectrometer of reasonable size. A resolution of 1000 is NOT achievable in a spectrometer th will fit in the space envelope provided.

5) The filtering for the instrument will consist of a long pass filter (>200 um) as far upstream as possible in the optical train (i.e. this could be the slit for the spectrometer and the entrance to the 4K box for the photometer). There will be a "thermal" short pass filter (<600 um) at 2K for both channels to reject the 4K radiation. There will be band pass filtering as close as possible to the detectors as appropriate for photometery and spectroscopy.

6) There will be a design workshop at the end of June 1997 (25,56,27) at whic the design of the instrument for the response to the AO will be finalised. This will be at RAL.

---

5) Colin Cunningham has been asked to co-ordinate inputs into the IID.

FIRST BOL GRATING MEETING: QMW 9/5/97

BOL/QMW/M/0017.1

NAME	INSTITUTION	TELEPHONE / FAX	E-MAIL
SYE MURRAY	QMW	0171-975-5010 (TEL.)	a.g.murray@qmw.ac.uk
Bruno MAFFEI	QMW	0171-975-4039	b.maffei@qmw.ac.uk
P. ADE	"	" " 5032	P.A.R.ADE@ "
I Hepburn	MSSL	01483 204101	IDH@MSSL.UCL.AC.UK
PETER HASTINGS	ROE	0131 668 8226 phone 668 1130 fax	prh@roe.ac.uk
WILLIAM DUNCAN	OI	01865 887855 881567 fax	william.duncan@oxinst.co.uk
KJETIL DOHLEN	OM	+33 4 95 04 41 24	
EC Attard	ROE	FAX: 91 62 11 90 0131 668 8207	
COLIN CUNNINGHAM	ROE	email: cca@roe.ac.uk 0131 668 8223	CRC@ROE.AC.UK
Matt Griffin	QMW	0171-975-5068	m.j.griffin@qmw.ac.uk
Tony Richards	RAL	01235-446146 Tel -445848 FAX	A.G.RICHARDS@RL.AC.UK
BRUCE SWINYARD	RAL	01235-446605 OR 446667 FAX	B.M.SWINYARD@RL.AC.UK.

QUESTIONS THE MODELS MUST ANSWER.

NEXT MTG = 13/6/97 FOR DISCUSSION ON 25/6/97.

- INPUT SLIT DIFFRACTION CALCULATIONS (WDD)
- ASAP + STRAYLIGHT ANALYSIS OF PHOTOMETER (WITH EA'S LATEST DESIGN). (TR) NEXT MTG.
- CAN THE GRATING BE MADE - WHAT RMS. SURFACE ERROR. (B. BACH → KD TO CONTACT) 30/5/97
- IRTS/FICM GRATING (BMS TO CONTACT NAKAGAWA) 12/5/97
- OTHER MANUFACTURERS FOR DIFFICULT ASPHERIC MIRROR AND GRATING. (KD, BMS) NEXT MTG.
- KD TO CONTACT PETIT RE GRATING EFFICIENCY NEXT MTG.
- ALIGNMENT TOLERANCES (KD, EA). (NEXT MTG)
- SIZE OF CAMERA MIRRORS (EA). (NEXT MTG)
- CROSS DISPERSER DESIGN (BMS) (30/5/97). (KD + EA)
- PIEZO ELECTRIC GRATING DRIVE (FAZA). (NEXT MEETING) (2)

Summary of Discussion
9/5/97 Boc Grating Group

(1) Photometer Design "Frozen" on Eli's Design of May 1997
- ⇒ Straylight + Diffraction Limited Analysis now Required.
- ⇒ But F/7.4 and R=3.5m. FOV ≈ 5.2°. ⇒ ESA

(2) Two Reasonable Spectrometer Designs ⇒ Planar
- ⇒ Concave "Gregorian"

(3) Cross Disperser offers some advantages (Large multiplex advantage) at cost of some complexity
- ⇒ Further Design Studies Required.

(4) R=500 ≤ Achievable on Principle
R=1000 Looks difficult in the space available.

(5) Few days in June 25, 26, 27
Weds – Fri.
@ RAL.

- OVERALL ALIGNMENT BUDGET BETWEEN INSTRUMENT + SATELLITE (EA)
- END TO END PERFORMANCE MODEL (BMS CO-ORD) → MATHCAD. (REPORT NEXT MTG)
- FILTERS – SW CUT ON 200μm. LW CUT OFF 600μm [SPECTROM. + PHOTOMETER.] + BANDPASS FILTERING ON FRONT OF DETECTORS.
- ESTIMATES OF THROUGHPUT PER FILTER (PARA)

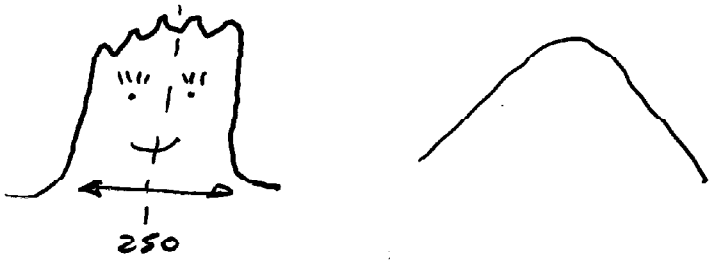

TITLE: **Curved grating optical design for spec-bol.**

PREPARED BY: **Martin Caldwell**

SUMMARY
An initial study of this design was included in the previous note on optical designs for spec-bol (2-4-97). Here the design is progressed to address aberration problem areas, in particular the correction of the large astigmatism, by means of an added fold mirror.

The design shown is not aberration-corrected nor optimised, as some changes in the resolution requirement & geometry are still required if the design is to fit the detector geometry. The purpose here is to pursue the conceptual design to help identify any show-stoppers before the detailed design is attempted.

The results for predicted system performance are given in the table on the last page, in terms of the net PSF spot size.

1. Design concept.
In this design, the entrance slit and detector array are placed on the Rowland circle of the grating, as shown in fig.1.

(5)

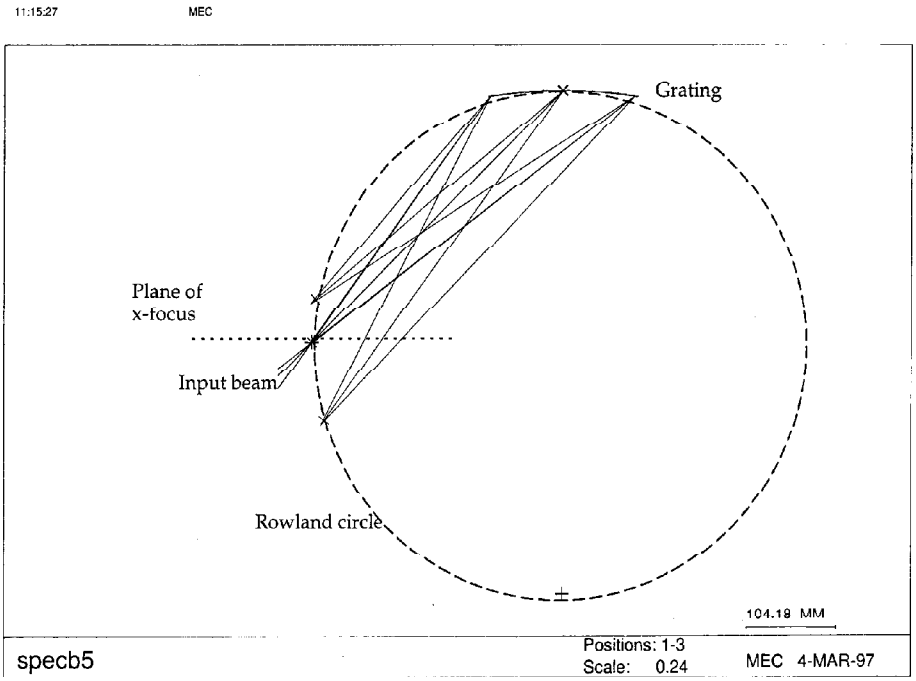

Fig.1. Curved grating design, in yz plane.

The initial design has the following parameters (Ref.1).

Centre wavelength: 0.3205mm, order 5.
Grating AOI: 45 deg.
Grating length: 200 mm
entrance relative aperture: F/3 circular
relative aperture at detectors : F/3
slit width : 0 (i.e. real value TBD)
grating scan range: + 1 deg.
pupil plane near grating.
Diffraction angle range: 45 deg. -5 deg. to +9 deg.
Imaging in cross-dispersion direction: not required.

2. Aberration effects.

The design is based on 19 detectors equally spaced in angle (ref.1), giving a spacing of approx. 7.7mm. This is close in compatibility with the minimum allowable

detector spacing of 5mm (giving detector active area diameter of 4mm, due to Winston cone geometry).

The imaging requirement is that the PSF central energy lobe fits within a diameter of approx. 4mm (although some relaxation of this requirement may come out as a result of further refinement of system resolution trade-offs).

At these wavelengths the Airy disc diameter is a few mm (see table below), and this means that a similar size can be allowed for the geometric aberration spot size. We list below the aberration effects, noting which are correctable and which are not.

Since the requirement for imaging in the along-slit direction (x-direction) has now been dropped, the imaging requirement in this direction is determined only by the light collection requirements of the detector. The imaging in the dispersion direction (y-direction) affects the spectral resolution, and this is likely to give a more stringent requirement. For now the requirement is taken as that quantified above.

2.1 y-direction effects.

Grating spherical aberration. This arises in the dispersion direction due to the use of a constant period grating, but it can be corrected using a varying-period grating (ref.2).

Scan-induced defocus.
As the grating is scanned by +1 degree, the Rowland circle (nominal focal point) moves laterally across the detector. Because the grating is not used at normal incidence, this motion produces a defocus in the beam on the detector. The size of defocus increases with the scan range, the relative aperture, and the grating angle of incidence used. For the current design the spot size increase due to scanning is by 1.25mm at the -5 deg. end of the array and by to 1mm at the +9 deg. end. This contribution is included in the table.

2.2 x-direction effects.

Rowland circle astigmatism.

In order to focus the beam in the x-direction (that perpendicular to the plane of the diagram), the grating must be toroidal. In the plane of the diagram the focusing is correct over all diffraction angles, due to the properties of the Rowland circle configuration. In the x-direction however, the focal plane is tilted, at 45 degrees to the output beam axis of the nominal design wavelength, as shown in the figure. This means that for diffraction angle positions other than the central one, there is astigmatism present, increasing with diffraction angle variation from 45 degrees. On the Rowland circle this leads to a severe defocus in the x-direction, of approx. 60 mm for the +9 degree position and 30mm for the -5 degree.

The astigmatism would be reduced by operating the grating at an incidence angle closer to the normal, or by reducing the aperture, but both of these give a loss of spectral resolution.

An alternative is to add extra optics to correct the astigmatism of the output beam. In the scheme shown in fig.2, a fold mirror is added in the output beam. The concept is that this mirror acts as a field mirror, by having an x-direction curvature which varies continuously in the dispersion direction. In the y-direction the mirror has no curvature. Denoting the dispersion angle relative to the Littrow position as δ, the mirror x-direction optical power is positive at δ=-5, becomes close to zero at δ=0 and then negative at δ=+9. This gives a 'fluted' shape to the mirror. So far the mirror form has been taken as an on-axis conic form, and this corrects of the astigmatism to a level where the x-direction spot size is < 10mm. The remaining aberration is chiefly spherical aberration due to the non-ideal form of the fold mirror used; the ideal form is an off-axis hyperbola, and use of this should allow the remaining aberration to be eliminated.

Aberration due to grating tilt.

In fig.2 the grating has been tilted in the x-direction to allow for accommodation of the fold mirror. In this diagram, there is still significant aberration evident. This is because of

1. To residual aberration of the non-ideal fold mirror as described above.
2. The grating form is left as toroidal, which is also non-ideal. To remove aberrations the form should be that of a toroid, having y-direction curvature circular and x-direction curvature elliptical.

Both of these aberration corrections can be added in the next iteration.

Aberration due to continuous form of fold mirror.

For any given detector, the fold mirror form can be optimised to correct the x-direction aberrations, as described above. If the mirror could be very close to the Rowland circle, then full correction could be made, but in the practical position some 10cm ahead of the detectors, there is some overlap between the beams from each detector. This feature, combined with the continuous nature of the optic, means that for a given detector it cannot give correct focusing at both the centre (paraxial portion) and the edge of the beam, and so spherical aberration is produced as follows.

The mirror is designed to have x-direction power which is correct for the paraxial detector beam (i.e. the centre of the beam) at each point, and the x-direction focal length as a function of angle, is denoted $f(\delta)$. The object distance for x-direction paraxial focusing is denoted $uo(\delta)$ and the image distance $vo(\delta)$. The image distance for the beam edge is denoted $v(\delta)$. The geometric spot size due to the differing image distances vo and v is given by

$$wx(\delta) = [vo(\delta)-v(\delta)]/F$$

(6)

where F is the f-number. v is given by the lens equation:

$1/v(\delta) = 1/f(\delta - \delta s(\delta)) - 1/u(\delta)$

where δs is the angular radius of the beam footprint on the fold mirror, as seen from the grating. To minimise this aberration, the fold mirror should be as close to the detectors as possible, but it cannot be less than approx. 10cm without the required optical power (and hence detector relative aperture) becoming excessive.

The above equations give values for wx which increase with increasing δ, due to the increasing size of the beam footprint on the fold mirror as its distance from the Rowland circle increases. The values range from approx. 1mm at δ=-5 up to 6 mm at δ=+5 and 20mm at δ=+9, as shown in the table. These sizes are too large to meet the requirements, and so some change in geometry would be required to make the design acceptable.

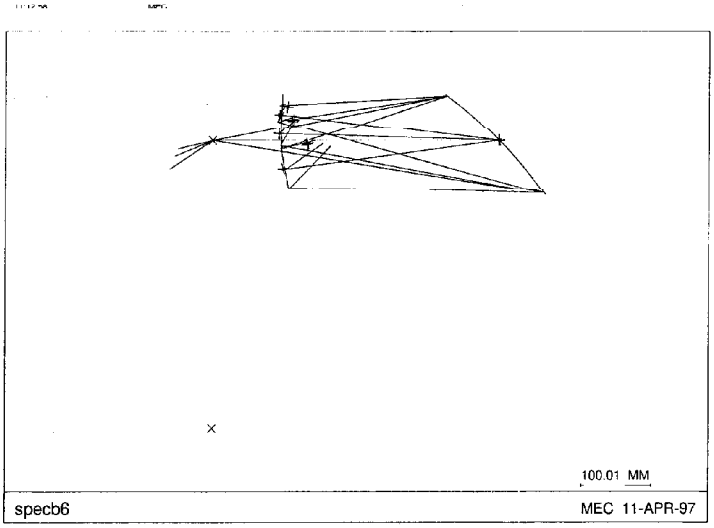

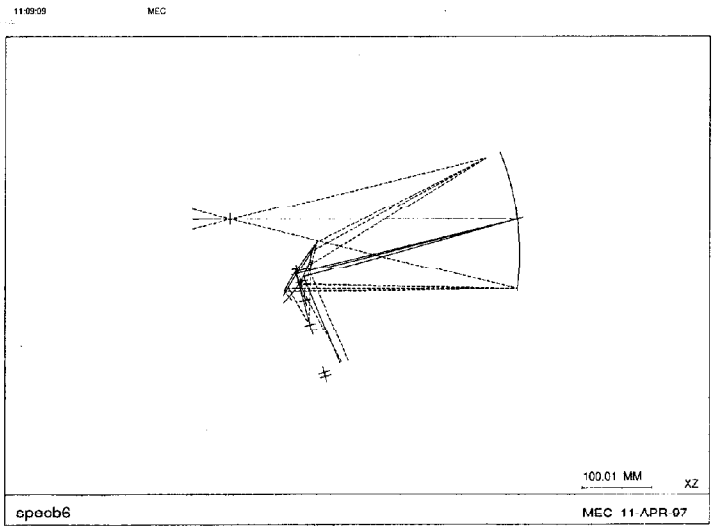

Fig.2 Curved grating design (not aberration corrected). Plan view (top) in plane of Rowland circle. Side view (bottom).

3. Expected performance.

The table below shows the expected approx. spot sizes for the design, after the correctable aberrations have been removed.

Summary of expected performance.

Effect	-5 deg.	+5 deg.	+9 deg.
Diffraction spot diam. (F/3 beam, (λ=209-350um))	1.5 - 2.6mm	1.5 - 2.6mm	1.5 - 2.6mm
Dispersion (y) direction scan-defocus	1.25mm	1.1mm	1mm
Cross-dispersion (x) direction aberration	1 mm	6 mm	20mm
Estimated total PSF spot size (Y x X) at longest λ	**3.8 x 3.6 mm**	**3.7 x 8.6 mm**	**3.6 x 20 mm**

4. Conclusion.

The main optical problem with this design is the aberration due to the continuous form of the fold mirror. The design might still be used over a limited range (e.g. -5 to +5 degrees), particularly if the following changes are made:

- Some ellipticity allowed in the detector geometry.
- Relaxation of resolution requirement (grating used at lower incidence angle / aperture reduced).

Also, the question remains as to whether this type of geometry would be suitable for the instrument thermal design and stray light budget.

References.

Ref.1 "Rowland circle option for the BOL spectrometer" B Swinyard Note F/N/009.01
Ref.2 *Diffraction gratings*. M. Hutley. Academic Press.

Preliminary Optical Design of BOL
Eli Atad , ROE , 9 May 1997

Photometer / Imager

- Working wavelengths: 200-600 microns
- Fnumber: F/5
- Field of View: 6.7 arcmin
- Chopper in the instrument and placed at the image of FIRST secondary mirror which is the stop of the telescope.
- Has to fit with the spectrometer in the 700*300*300 mm space enveloppe.
- A physical cold stop at 4K to reduce background radiation.
- The photometer will share the same foreoptics as the spectrometer (one chopper only, weight)
- 3 arrays of detectors optimized for 3 separate wavelengths: 250, 350,480 microns .
- No Filter wheel .

09:57:20

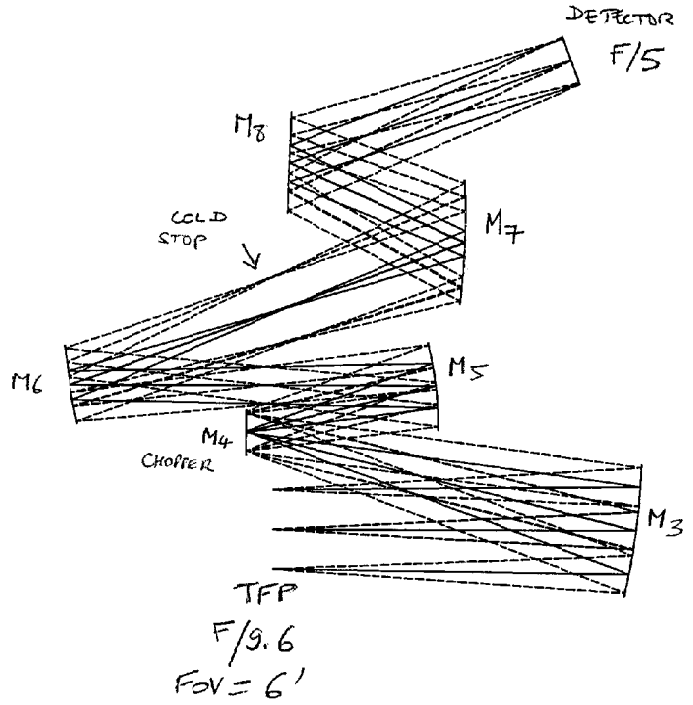

100.00 MM XZ

FIRST BOL PHOTOMETER/IMAGER Scale: 0.25 7-May-97

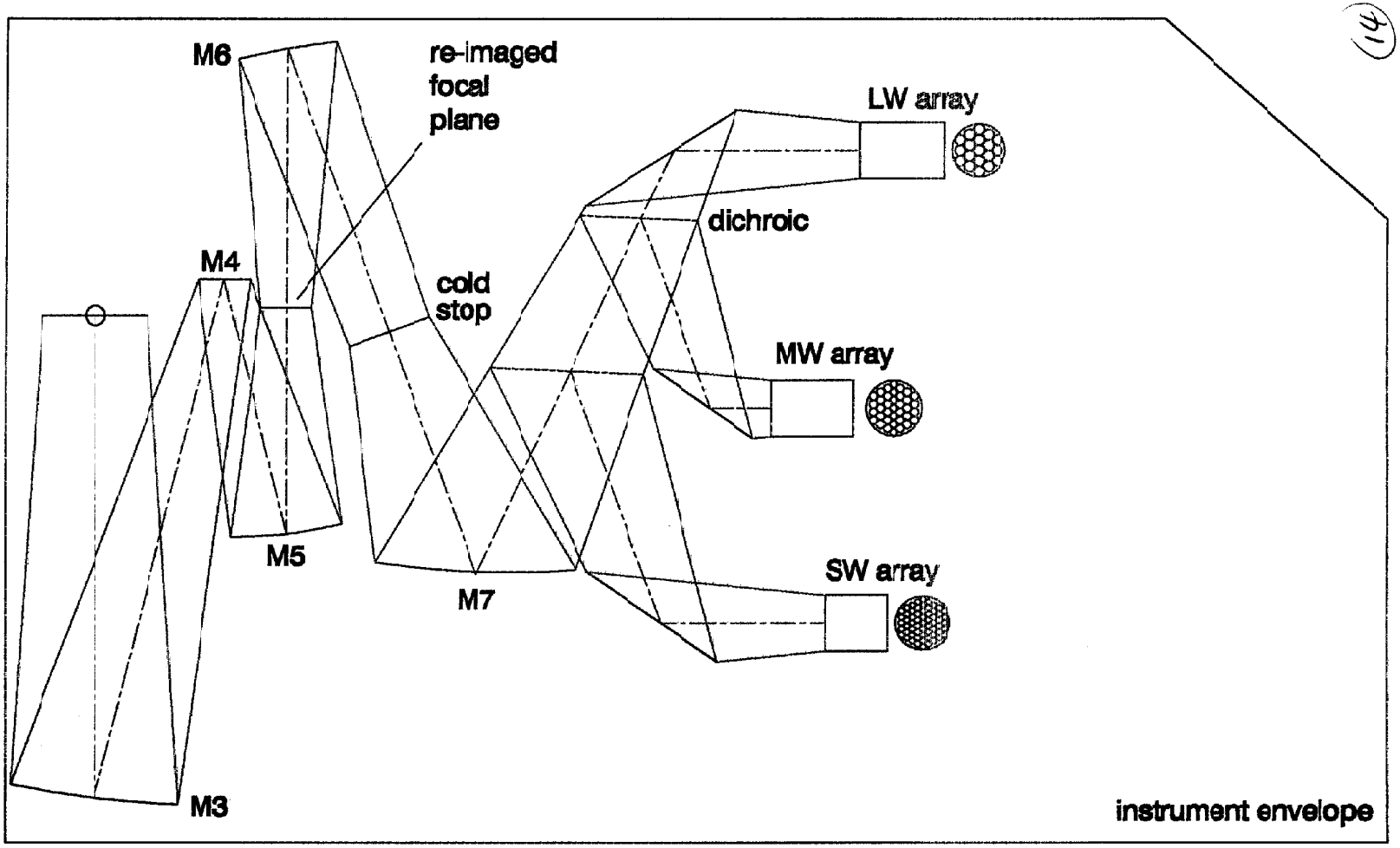

BOL photometer
f/5 final beam size
dichroic angle - 22.5 degrees

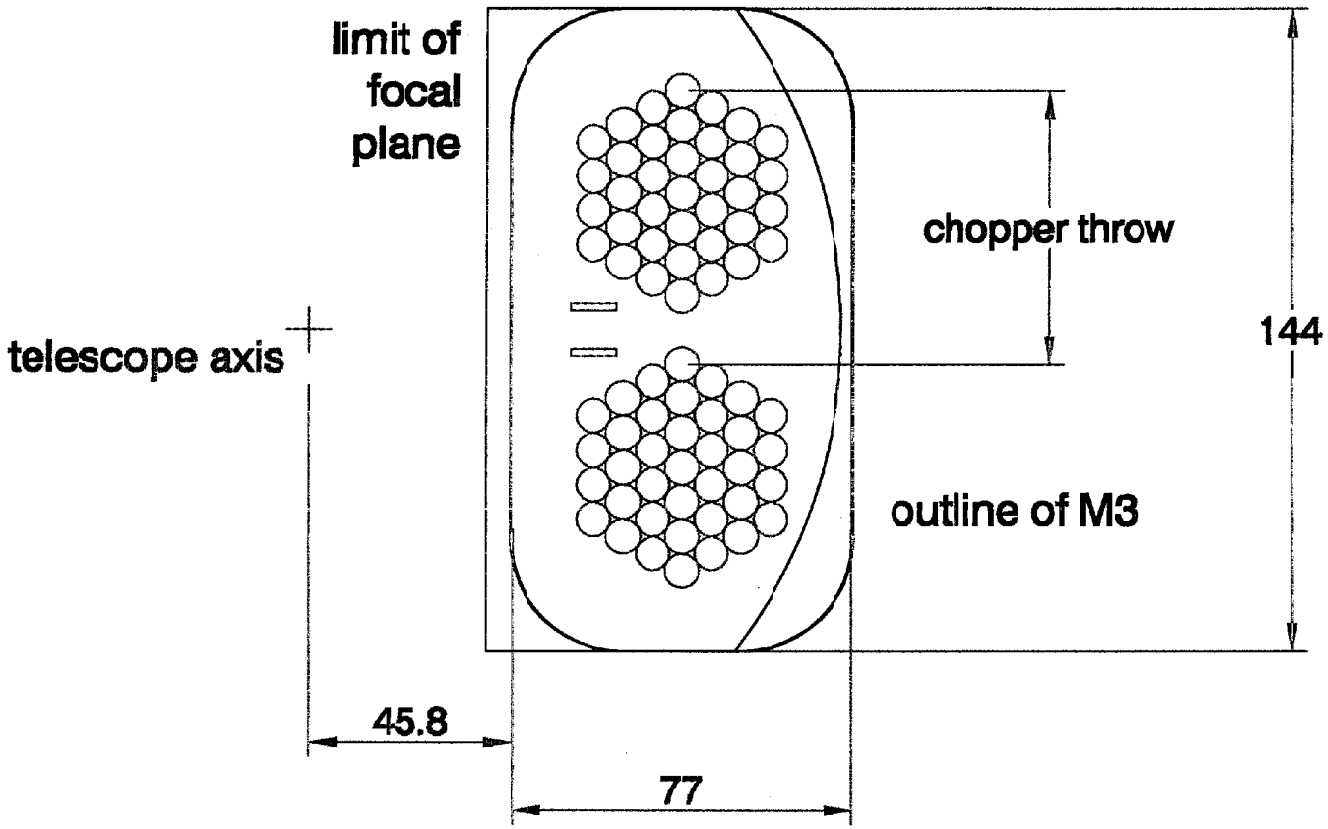

BOL instrument
spectrometer slit and
photometer detector array
mapped to the telescope focal plane

Photometer/Imager Optical Data:

Component	Radius of Curv (mm)	Thickness (mm)	y- Tilt (degrees)	CA Diameter (mm)
telescope FP f/9.5915 (7.64"/mm)	plano	240		53.0
M3	480.00	266.42	6.0	85.0
M4 (chopper)	plano	128.83	14.0	28.0
M5	224.0	112.0	7.0	86.0
cold reimaged focal plane	plano	129.18		
M6	470.77	177.34	10.0	30.0
cold stop	plano	100.0		28.0
M7	Ry= 377.8 Rx=448.3	127.0	22.0	72.0
M8 (dichroic)	plano	198.0	22.0	66/45
detector/f/5				25
(14.66"/mm)				

IMAGE QUALITY

Encircled Energy Diameters (mm) and Strehl ratios:

Wavelength (μm)	250	350	480
Airy disk (80%) (mm)	2.5	3.5	4.8
Geometrical spots (mm)			
80% on-axis	0.40	0.40	0.40
off-axis	1.4	1.4	1.4
Strehl ratios			
on-axis	1.0	1.0	1.0
off-axis	0.88	0.93	0.97

THROUGPUT : 0.89 (without filters)

(assuming 0.98 reflectivity per mirror)

Optical Design of BOL Spectrometer

- FOREOPTICS

The spherical collimator mirror M3 reimages the telescope pupil onto the chopper M4. A spherical concave mirror M5 reimages the slit focal plane onto a cold slit (4K) at ~f/4.5 (16.28 "/mm).

The diffraction (80%) of the telescope is $2*\lambda/D$ where D=2815 mm ; so for λ=200 μm , the Airy disk for the telescope is 29.3"/mm.The width of the slit , matching the diffraction of the telescope is about 1.8 mm.

The 3 mirrors in the foreoptics are at 20K. The input slit to the spectrometer is at 4K.

- COLLIMATOR:

A spherical concave mirror sends a 120 mm collimated beam to the grating and also reimages the pupil onto the grating to avoid changes in scattering by the grating along the slit.

- GRATING:

Quasi-Littrow configuration. Blaze angle: 40 degrees, Blaze wavelength: 275 μm; order 4 ; groove spacing: 0.925 mm off-axis angle: 44 degrees ; grating movement: ±1 degree Size: 200 mm

- CAMERA (F/3):

2 tilted concave mirrors . An intermediate physical image of the slit spectrum will allow the insertion of a cold mask at 4K, to stop straylight and diffraction effects from the grating

15:03:18

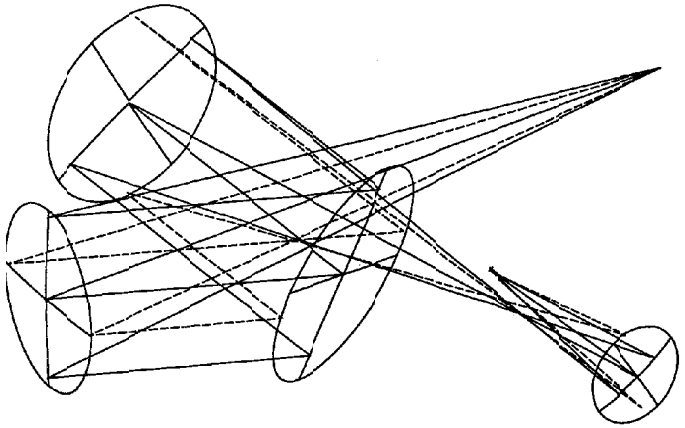

100.00 MM

FIRST BOL SPECTROMETER Scale: 0.25 8-May-97

BOL SPECTROMETER OPTICAL DATA

Component	Radius of Curv (mm)	Thickness (mm)	y- Tilt (degrees)	CA Diameter (mm)
telescope FP f/9.5915 (7.64"/mm)	plano	240		53.0
M3	480	266.42	6.0	85.0/25.0
M4 (chopper)	plano	128.83	12.0	28.0
M5	224.0	112.0	6.0	56.0/25.0
slit at ~f/4.5 (16.28"/mm)	plano	537.0		25.0
M6 Collimator	1074.0	200	15.0	130.0
Grating (40 deg./5th order/)	plano	200	40.0 x-tilt: 22 deg.	200.0/130.0
Cam1	Ry=961.7 k= -6.57	392.355	15.0	
slit image	plano	257.645		
Cam2	Ry = 144.79 Rx= 175.92	147.7	10.0	
detector/horn f/3 (24"/mm)				

SPECTRAL RESOLUTION

Grating tilt θ (degrees)	40	40
λ (microns)	275	350
order	4	3
dispersion (mm)	0	-22
R= 240* tgθ/λ (theoretical limit)	732	575
R=2* tgθ* Fcam/a a=pixel size=2mm Fcam=360mm	302	302

IMAGE QUALITY

Encircled Energy Diameters (mm) and Strehl ratios:

Dispersion (mm)	0	22
Wavelength (μm)	275	350
Airy disk (80%) (mm)	1.65	2.1
Geometrical spots (mm) 80% eed	1.70	2.5
Strehl	0.90	0.85

througput: 0.67 (including 0.80 for grating and 0.98 for mirrors)

2/5/97

Aberration corrected concave grating for SPEC-BOL

Kjetil Dohlen

Laboratoire d'Optique, Observatoire de Marseille
2 Place Le Verrier, 13248 Marseille Cedex 4, France

1. INTRODUCTION

For the spectroscopy channel of the FIRST bolometer instrument (SPEC-BOL), it has been agreed during the last BOL work-group meeting in Edinburgh (3/4/97) that:

1) No imaging is required (except perhaps two rows of detectors)

2) The grating should have a very small movement, only a couple of degreesm

3) Many detectors (~20) with individual order sorting filters

4) Up to 150 mm long line of detectors

5) Minimum horn aperture 2.5 mm, physical outer diameter 4.5 mm, but could be bigger

6) Slit must not be narrower than an Airy disc diameter for optimal throughput and to limit diffraction effects

7) Horn apertures should not be narrower than Airy disc diameter for optimal throughput

8) Cold stop in a pupil plane close to the detectors required

The effects of this upon the optical concept may be summarized as:

Type of spectro:

The instrument becomes more of a *spectrograph* than of a *monochromator*: the row of detectors covers a wider angular range than the angular movement of the grating.

Resolving power:

The instrument will have slit-limited rather than diffraction-limited resolving power. In order to obtain the diffraction limit, both slit and detector aperture (exit slit) should have angular widths of about λ/D_G (D_G is width of the diffracted beam) instead of $2.44\lambda/D_G$ as dictated by the Airy disc diameter. Since the slit width cannot vary with wavelength, the slit-limited resolution is given by the longest wavelength observed.

Note however that for unresolved objects, the object itself defines the effective slit and the physical slit size is unimportant. Higher resolving power may then be achieved for shorter wavelengths by reducing the horn size proportionally with wavelength. Nevertheless, we do not propose this possibility here because of limited aberration correction.

Cold stop:

If there is a pupil image on the grating and we need another pupil image before the detector for the cold stop, then, by first-order optics, it is necessary to produce an intermediate spectral image as well. A Gregorian-style camera with a flat grating will provide this as shown in Caldwell's design. However, for the very long spectral image required, the size of the first camera mirror becomes very large. Swinyard proposed using a concave grating, putting the cold stop on the grating itself. Problems with astigmatism in his Rowland circle design were prohibitive however. Also, the cold stop would be big and move with the grating.

Proposed solution:

I here propose to use a different type of concave grating allowing better aberration control. Also, I propose to reimage the spectrum produced by the grating via a concave mirror, thus producing the required fixed cold-stop.

(22)

2. OPTICAL CONCEPT

A concave grating (G) with a slit in A produces a real spectral image in B, see Fig. 1. Reimaging this spectrum via a concave mirror (C) produces an image of the grating (CS) in front of the detectors (D). If the grating is in a pupil plane, CS is also in a pupil plane, providing the ideal location for a cold stop. If a field stop is located in B, it seems the system may be very well baffled.

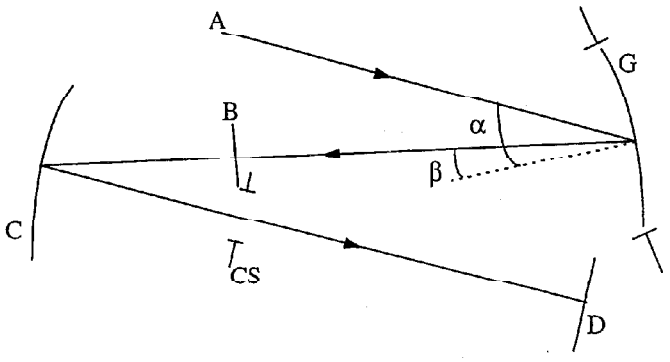

Figure 1. Concept sketch. A: slit, G: concave grating, B: intermediate spectrum, C: concave mirror, CS: cold stop, D: detectors, α: angle of incidence, β: angle of diffraction.

The couple G+C is equivalent to a flat grating with a Gregorian-style camera, except that the primary of the Gregorian is fused into the grating, as is the collimator. A penalty for this is that even a small variation in the grating angle, required for spectral scanning, degrades significantly the image quality of the system. Spectral scanning is therefore obtained by tilting C.

For CS to be accessible, the focal ratio of the camera (F_C) must be larger than that of the grating (F_G). Since F_G cannot reasonably be much smaller that 2, we are limited to an F_C of 4-5. Although larger than earlier specified (F_C~3) this does not seem to be a disadvantage since detector horns then become larger and the dead area between detectors due to filter supports etc. becomes smaller.

2.1 Grating design

From the grating equation:

$$\sin\alpha + \sin\beta = n\lambda/d \tag{1}$$

and its derivative:

$$d\beta \cos\beta = nd\lambda/d\,, \tag{2}$$

resolving power may be given by:

$$R = \lambda/\Delta\lambda = \frac{\sin\alpha + \sin\beta}{\Delta\beta \cos\beta}\,, \tag{3}$$

where $\Delta\beta$ is the angular size of the detector seen from the grating. For diffraction limited resolving power, $\Delta\beta$ is taken to the FWHM of the Airy peak, i.e. $\Delta\beta = \lambda/D_G$, where D_G is the width of the grating projected onto the normal to the diffracted beam. However, as explained above, we are obliged to take $\Delta\beta$ equal to the *diameter* of the Airy disk at the longest wavelength, ie.:

$$\Delta\beta = 2.44\lambda_{max}/D_G. \tag{4}$$

Linear dimension of the detector aperture is given by:

$$\Delta x = f_C\Delta\beta, \tag{5}$$

where f_C is camera focal length. Focal ratio of the camera beam is:

$$F_C = f_C/D_G. \tag{6}$$

The proposed system has a final focal ratio of $F_C = 4$ and a projected diameter of the grating of $D_G = 185$ mm, giving a focal length of $f_C = 740$ mm. Angular detector aperture is calculated by eq. (4) for $\lambda_{max} = 350$ μm to $\Delta\beta = 0.26°$, corresponding to 3.4 mm in the focal plane according to (5).

In the present design, angle of incidence at the grating is $\alpha = 45°$ and mean diffraction angle is $\beta = 30°$. Actual, detector limited resolving power is therefore, by eq. (3), R = 307. It may be possible to increase α and β toward 55° and 40°, respectively, obtaining R ~ 420, but it seems that aberration correction is the limiting factor.

Due to the departure from the Littrow condition, the diffracted beam cross-section is slightly oval giving an F-number of 4.9 in the non-dispersed direction. Fitting the Airy disk into the detector in this direction therefore requires an aperture of 4.2 mm. The circular horns should therefore have this aperture diameter and be fitted with a rectangular mask providing the 3.4 mm spectral aperture. Allowing for a 1 mm ring around the aperture to hold the filter, the centre-to-centre detector separation is 6.2 mm, corresponding to an angular separation of 0.44°. I assume in the following an angular detector separation of 6.5 mm or 0.50°.

2.2 Spectral output

The spectrum is dispersed onto a line of 18 detectors covering 117 mm in the focal plane. Shifting the spectrum with respect to the detectors by ±4 detector separations ensures coverage of the required spectral band of 200-350 μm using orders 10-16 as shown in Table 1. At the current resolving power this leaves 5 spare detectors which may be used to obtain intermittent spectral coverage up to 500 μm (shown in italics in the table).

Working in high orders is necessary to limit the width of the detector array and hence allowing acceptable aberration correction. Order-sorting filters have resolving powers of 15-20.

The spectral shift could be achieved by a ±1° rotation of the grating, but this introduces an intolerable increase in aberrations. Instead, the shift is produced by a ±1.5° rotation of the camera mirror with only a negligible change in aberrations as will be shown below.

Table 1. Distribution of the spectral range from 200 to 350 μm over the 18 individually filtered detectors. The range index numbers the pieces of spectrum sequentially from long to short wavelengths. The detector index numbers detectors from one end to the other of the focal plane.

Range index	Detector index	Order	Wavelength range Min	Max
1	*17*	*7*	*476.24*	*498.64*
2	*14*	*8*	*409.13*	*429.07*
3	*3*	*8*	*380.37*	*401.43*
4	*13*	*9*	*361.40*	*379.22*
5	*4*	*9*	*340.48*	*359.12*
6	18	10	335.37	350.96
7	10	10	319.07	335.37
8	2	10	302.15	319.07
9	9	11	288.17	303.06
10	16	12	276.13	289.28
11	8	12	262.41	276.13
12	1	12	250.00	264.16
13	6	13	238.99	251.77
14	11	14	229.39	240.97
15	15	15	219.56	230.13
16	7	15	208.53	219.56
17	12	16	202.00	212.08
18	5	16	192.85	203.29

2.3 Optical design

Figure 2 shows a perspective view of the proposed spectrometer and Table 2 summarizes the optical design. The fore-optics transforming the telescope F/9.5 beam into the F/2.2-beam required by the spectro is not yet designed, but it will probably consist of two powered mirrors following the M4 pupil-chopping mirror, plus a small folding flat just after the slit. Since the chopper will probably be shared with the photometer, the fore-optics design depends upon the photometer design.

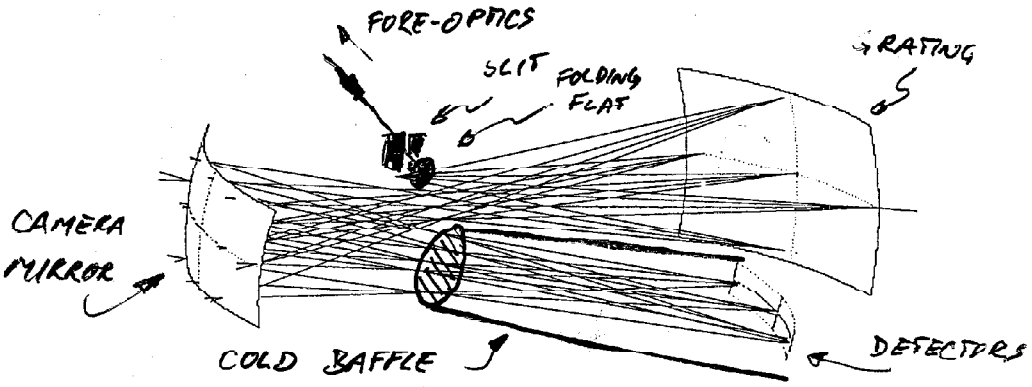

Figure 2. Perspective view of the proposed system. The slit is coplanar with the intermediate spectral image and the final image is folded below this plane. The pupil image accessible for a cold stop is just below the intermediate spectral image. Scale of the drawing is approximately 1:5, distance between grating (on the right) and camera mirror (on the left) is 500 mm.

Table 2. Summary of the optical design. All dimensions are in mm unless otherwise stated.

Surface	Radius	Notes	Size	Separation
Slit			Width: 1.9	325
Grating	-357.36	Mean gr. const.: 0.39 g/mm	220 x 160	-300
Intermediate spectrum				-200
Camera mirror	285.00	Deformation: R^4: 9.87e-10 y^2: 1.17e-5 R^4y: -2.33e-11 y^3: 6.18e-7 R^4x: 9.97e-12 x^3: 5.90e-7	230 x 110	200
Cold stop			Oval: 75 x 61	300
Detectors	-307.00	Horn spacing: 6.5 Horn ap. dia.: 4.2 Mask width: 3.4	Length: 117 (18 detectors)	

Grating

A spherical substrate is used for the grating, but the rulings are unequally spaced, as shown in Figure 3 (filled-in circles). In the optimized system the rulings are also non-parallel, but as shown in Figure 3 (hollow circles) the departure from parallelism is small and perhaps not essential. The grating constant varies between 0.37 g/mm and 0.40 g/mm. Note that while the grating is simulated as a holographic grating generated with two interfering point sources, it will most probably be manufactured by mechanical ruling or machining. Which additional constraints and/or freedoms this gives with respect to substrate and groove shape are currently unknown, see Sec. 2.5.

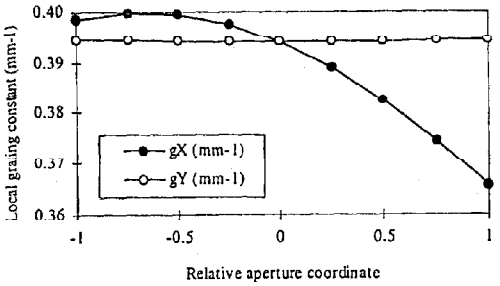

Figure 3. Variation of grating constant across the grating in the spectral direction (filled-in circles) and in the non-spectral direction (open circles).

Camera mirror

An intermediate spectral image is produced next to—and co-planar with—the slit. The camera mirror relays this image onto the final spectral image at a focal ratio of F/4 in the dispersion direction and F/4.9 in the non-dispersion direction. Although the main reason for introducing the camera mirror was to obtain a real pupil image in front of the detectors, it has also proven essential in obtaining sufficient aberration correction. This has been achieved by heavily deforming the mirror. Figure 4 shows a contour map of the surface deformation (sphere subtracted) and Figure 5 shows x and y profiles. The mirror aperture is rectangular and slightly offset from the vertex as shown in Figure 4, reaching from -125 mm to +105 mm in the dispersion (x) direction and from -55 mm to +55 mm in the non-dispersion (y) direction. As seen in Figure 5 the main deformation is an S shape in the x-direction produced by an x^3 function.

The focal surface is concave with a radius of about 300 mm which makes it concentric with the cold stop. All rays are therefore normal to the focal surface which I suppose is an advantage for the layout of the detector horns.

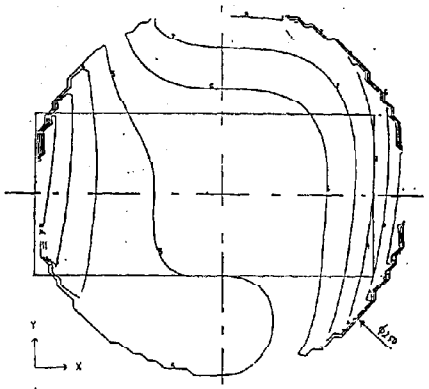

Figure 4. Contour map of the deformation of the camera mirror. Contour increment is 0.3 mm The rectangular aperture of the mirror is shown. Dispersion direction is horizontal.

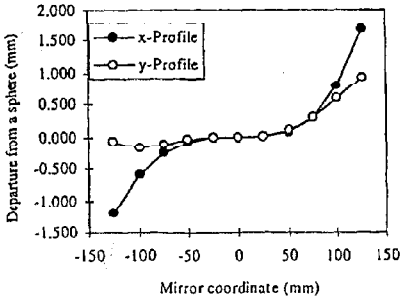

Figure 5. Profiles of the deformation of the camera mirror in the dispersion direction (filled circles) and in the non-spectral direction (open circles).

2.4. Optical performance

Fig. 6. shows spot diagrams for the wavelength range covered by the 10th order (300-350 μm). Five different wavelengths (300, 312, 325, 338, and 350 μm) are traced for three scan positions of the camera mirror (+1.5°, 0, and -1.5°). Spot positions are shown relative to the detector array. Corresponding wavelengths in the other orders have identical spots. Most of the spots are inscribed in the detector apertures, and with RMS wavefront errors ranging from 25 μm to 50 μm, the imaging is nearly diffraction limited for the longest wavelengths.

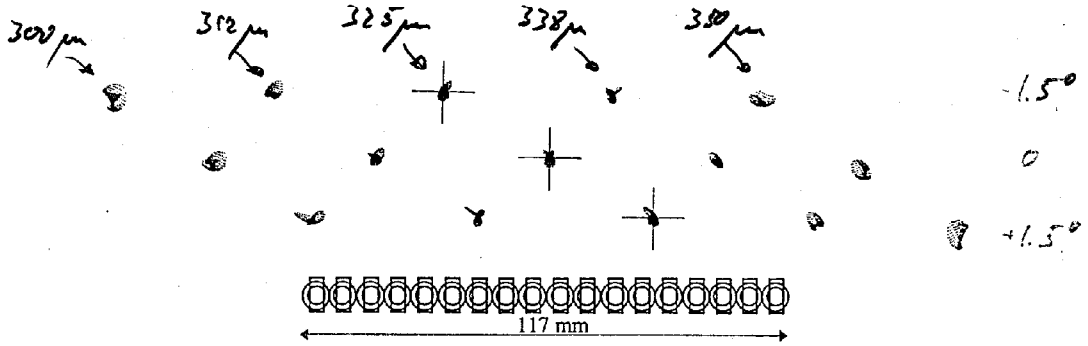

Figure 6. Spot diagrams for five wavelengths in the 10th order and three scan positions of the camera mirror are shown next to the detector array.

2.5. Fabrication and testing.

Dr. Bach of Hyperfine (LWS grating) has been contacted for the fabrication of grating and camera mirror. He will comment upon the feasibility on the basis of this note, but asked for an immediate impression, he said the testing appeared more of a concern than the actual machining. His approach will probably be as for the LWS case where interferometric tests where made at 10 μm.

Michel Saisse of LAS strongly advocates that an optical set-up allowing tests in the FIR range should be provided within the consortium.

3. CONCLUSIONS

An original, two-component spectrometer has been proposed for SPEC-BOL. Continuos spectral coverage with a slit-limited resolving power of 307 is obtained for the spectral range 200-350 μm as well as an intermittent coverage up to 500 μm. Increasing the resolving power towards 400 may be possible but optimization is delicate and the aberration correction will probably be the limiting factor.

Precision : 1-5 μm (TBC)

(27)

SPCRES13.XLS, Orders

18:31, 06/05/1997

nmin 8 no unit

d 2.70293 mm = 1/0.37 mm-1

alpha 45 deg

beta0 30 deg

dbeta	-6.5	-6	-5.5	-5	-4.5	-4	-3.5	-3	-2.5	-2	-1.5	-1	-0.5	0	0.5	1	1.5	2	2.5	3	3.5	4	4.5	5	5.5	6
beta	23.5	24	24.5	25	25.5	26	26.5	27	27.5	28	28.5	29	29.5	30	30.5	31	31.5	32	32.5	33	33.5	34	34.5	35	35.5	36
n																										
8	373.63	376.33	379.02	381.70	384.36	387.02	389.66	392.30	394.92	397.53	400.12	402.71	405.28	407.84	410.39	412.92	415.44	417.95	420.44	422.92	425.39	427.84	430.28	432.70	435.11	437.50
9	332.12	334.52	336.91	339.29	341.66	344.02	346.37	348.71	351.04	353.36	355.67	357.96	360.25	362.53	364.79	367.04	369.28	371.51	373.73	375.93	378.12	380.30	382.47	384.62	386.76	388.89
10	298.91	301.06	303.21	305.36	307.49	309.61	311.73	313.84	315.93	318.02	320.10	322.17	324.22	326.27	328.31	330.34	332.35	334.36	336.35	338.34	340.31	342.27	344.22	346.16	348.09	350.00
11	271.73	273.69	275.65	277.60	279.54	281.47	283.39	285.31	287.21	289.11	291.00	292.88	294.75	296.61	298.46	300.31	302.14	303.96	305.78	307.58	309.37	311.16	312.93	314.69	316.44	318.18
12	249.09	250.89	252.68	254.46	256.24	258.01	259.78	261.53	263.28	265.02	266.75	268.47	270.19	271.89	273.59	275.28	276.96	278.63	280.30	281.95	283.59	285.23	286.85	288.47	290.07	291.67
13	229.93	231.59	233.24	234.89	236.53	238.17	239.79	241.41	243.03	244.63	246.23	247.82	249.40	250.98	252.55	254.11	255.66	257.20	258.73	260.26	261.78	263.29	264.79	266.28	267.76	269.23
14	213.50	215.05	216.58	218.11	219.64	221.15	222.66	224.17	225.67	227.16	228.64	230.12	231.59	233.05	234.51	235.96	237.40	238.83	240.25	241.67	243.08	244.48	245.87	247.26	248.63	250.00
15	199.27	200.71	202.14	203.57	204.99	206.41	207.82	209.22	210.62	212.01	213.40	214.78	216.15	217.52	218.87	220.22	221.57	222.91	224.24	225.56	226.87	228.18	229.48	230.77	232.06	233.33
16	186.82	188.17	189.51	190.85	192.18	193.51	194.83	196.15	197.46	198.76	200.06	201.35	202.64	203.92	205.19	206.46	207.72	208.97	210.22	211.46	212.69	213.92	215.14	216.35	217.55	218.75
17	175.83	177.10	178.36	179.62	180.88	182.13	183.37	184.61	185.84	187.07	188.29	189.51	190.72	191.93	193.12	194.32	195.50	196.68	197.86	199.02	200.18	201.34	202.48	203.62	204.76	205.88
18	166.06	167.26	168.45	169.64	170.83	172.01	173.18	174.35	175.52	176.68	177.83	178.98	180.12	181.26	182.39	183.52	184.64	185.76	186.86	187.97	189.06	190.15	191.23	192.31	193.38	194.44
19	157.32	158.45	159.59	160.71	161.84	162.96	164.07	165.18	166.28	167.38	168.47	169.56	170.64	171.72	172.79	173.86	174.92	175.98	177.03	178.07	179.11	180.14	181.17	182.19	183.20	184.21
20	149.45	150.53	151.61	152.68	153.75	154.81	155.87	156.92	157.97	159.01	160.05	161.08	162.11	163.14	164.16	165.17	166.18	167.18	168.18	169.17	170.16	171.14	172.11	173.08	174.04	175.00
21	142.34	143.36	144.39	145.41	146.42	147.44	148.44	149.45	150.44	151.44	152.43	153.41	154.39	155.37	156.34	157.30	158.26	159.22	160.17	161.11	162.05	162.99	163.92	164.84	165.76	166.67
22	135.87	136.85	137.82	138.80	139.77	140.73	141.70	142.65	143.61	144.55	145.50	146.44	147.37	148.31	149.23	150.15	151.07	151.98	152.89	153.79	154.69	155.58	156.46	157.35	158.22	159.09
23	129.96	130.90	131.83	132.76	133.69	134.62	135.53	136.45	137.36	138.27	139.17	140.07	140.97	141.86	142.74	143.62	144.50	145.37	146.24	147.10	147.96	148.81	149.66	150.50	151.34	152.17
24	124.54	125.44	126.34	127.23	128.12	129.01	129.89	130.77	131.64	132.51	133.37	134.24	135.09	135.95	136.80	137.64	138.48	139.32	140.15	140.97	141.80	142.61	143.43	144.23	145.04	145.83
25	119.56	120.43	121.29	122.14	123.00	123.85	124.69	125.53	126.37	127.21	128.04	128.87	129.69	130.51	131.32	132.13	132.94	133.74	134.54	135.34	136.12	136.91	137.69	138.46	139.23	140.00

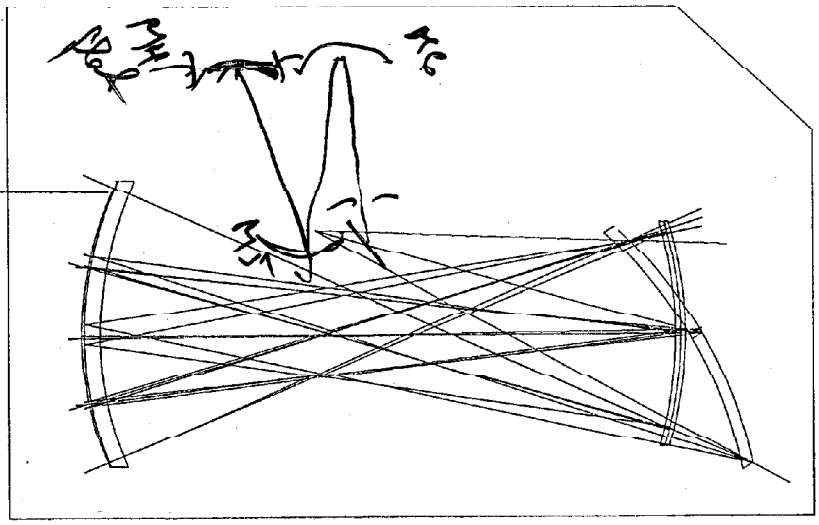

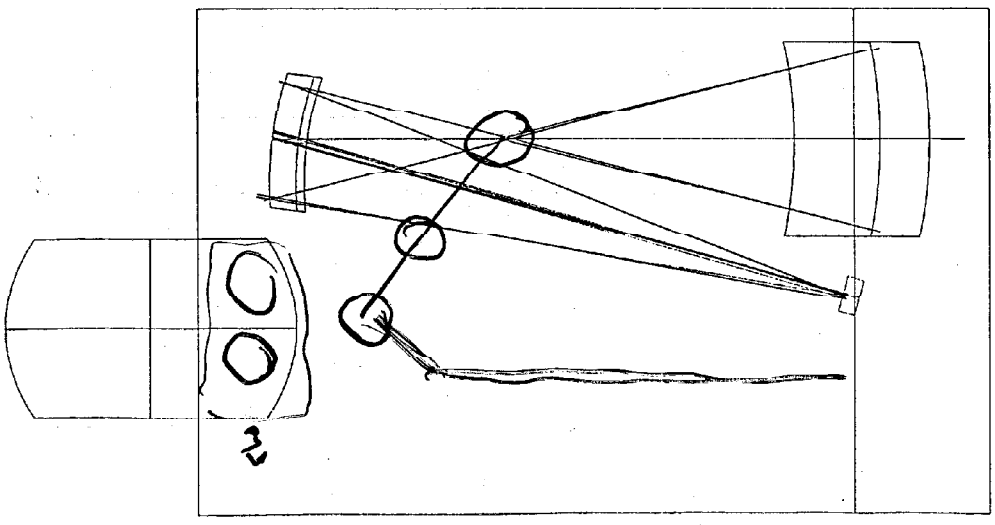

Introduction

On the issues that needs to be resolved before the design of the BOL spectrometer can be finalised is what resolution is actually achievable with a grating spectrometer of reasonable size in the 200 to 350 μm waveband. By reasonable size I mean "will it fit in the box"!. In this note I try to address this question by looking at what slit size is necessary to achieve a given resolution for a given grating dispersion and collimator focal length. I also try to address the affect of diffraction at the slit on the grating response function.

Slit Size

The dispersion of a grating is given by:

$$\frac{d\beta}{d\lambda} = \frac{m}{a\,\mathrm{Cos}\beta} \quad (1)$$

where m is the order, a the groove width and β the diffraction angle from the grating. Figure 1 shows the dispersion plotted as a function of input (α) and output angles (β) for both angles on the same side of the normal. The contours are for $\lambda d\beta/d\lambda$ - i.e. the true dispersion in radians/μm is obtained by dividing by the wavelength. The straight line represents the Littrow condition in which $\alpha = -\beta$.

If the width of the slit is set to be one resolution element (however defined!) and the focal length of the collimator is taken as the effective distance between the slit and the grating, then the slit width is given by:

$$W_S = \frac{mF_c\lambda}{Ra\,\mathrm{Cos}\beta} \quad (2)$$

where F_c is the collimator focal length and R is the resolving power. The three quasi-Littrow designs for the SPEC-BOL have used $\alpha = -\beta \approx 45°$; for these angles the dispersion is $2/\lambda$. Taking λ = 250 μm, figure 2 shows the slit width as a function of resolving power and collimator focal length. The two dotted lines are for R=500 and R=1000. If an f/3 ratio is used for the collimating optics then $2f\lambda$ is 1.5 mm - the minimum size required to have an efficient throughput. From figure 2 this slit size would require $F_c \sim 380$ mm for R=500 and $F_c \sim 750$ mm for R=1000; the aperture would correspondingly be 1/3 of these figures. Clearly the R=1000 case is going to cause some design difficulties in the SPEC-BOL given the restricted space available.

Slit Diffraction

The affect of diffraction by the slit can be examined by treating the amplitude pattern formed by the fore-optics and clipped by the slit as the Fourier transform of the far field amplitude pattern subsequent to the slit. The amplitude pattern of the fore-optics is given by:

$$E(q) = E(0)\left(\frac{2\,J_1(kq/2f)}{kq/2f}\right) \qquad (3)$$

where J_1 is a Besel function of first order, f is the focal ratio, $k = 2\pi/\lambda$ and q is the distance from the optical axis. I have used IDL to calculate this in two dimensions for f = 3 and then clipped the amplitude pattern with a slit of 1.5 mm. Taking the Fast Foruier Transform (FFT) of this and scaling the ordinate appripriately, one can calculate the far field intensity pattern beyond the slit as a function of angle. This is shown in figure 3 for two cuts; one along the central axis of the slit, and one across the central axis of the slit. One can see that the inesity pattern along the slit is more or less as one would expect for an f/3 beam (half angle 9.46°), but across the slit the beam shape is radically alterred and energy is diffracted well beyond the f/3 beam - i.e. it will miss the next optical surface and, therefore, presumably the grating.

Affect on Grating Response

This loss of energy will have an affect on both the efficiency and the spectral quality of the system. I have not studied the affect on the effiency in great detail as yet as there will be other complicating factors in this; however the affect on the spectral performance can be estimated by treating the grating as a multiple slit device and calculating the Fraunhofer diffraction pattern as follows (Hecht and Zajac):

$$E(\theta) = \sum_{j=0}^{N-1} C_i \left(\frac{\sin B}{B}\right) \sin(\omega t - kr + 2Bj) \qquad (4)$$

where $B = ka/2\,(\sin\beta - \sin\alpha)$, N is the number of grooves and C_j is the average intensity over the j'th groove. The grating response for an arbitray incident instensity pattern can then by calculated. Figure 4 shows the calculated grating response for the intensity pattern across the slit shown in figure 3 (solid line) and that for uniform illumination (dashed line) - both have been normalised to one at the maximum. It can be seen that the slit diffraction causes the width of the central maximum to increase slightly - in this case the resolving power goes from 1131 to ~ 820 - but the side lobes have been reduced substantially. When these responses are smoothed with "1.5 mm slit" - in fact a used a box car smoothing to simulate this! - the difference becomes even less dramatic - figure 5. The difference in resolving power between the two cases is minimal but the side lobes have still been suppressed for the diffraction limited case.

Conclusions

1. A resolving power of 500 is achievable in a reasonably sized instrument and the slit diffraction should not be a problem if the grating is suitably oversized. In the case tested a

grating capable of R=1131 easily delivered R=500 with oversized slits.

2. A resolving power of 1000 is much more difficult and probably rendered impossible by the diffraction at the slit.

The outstanding issues to consider are:

- What is the affect of slit diffraction on the throughput efficiency.
- What oversizing of the grating and/or optics is necessary to deliver R=500.

It will require a more sophisticated treatment - probably ASAP - to answer these questions.

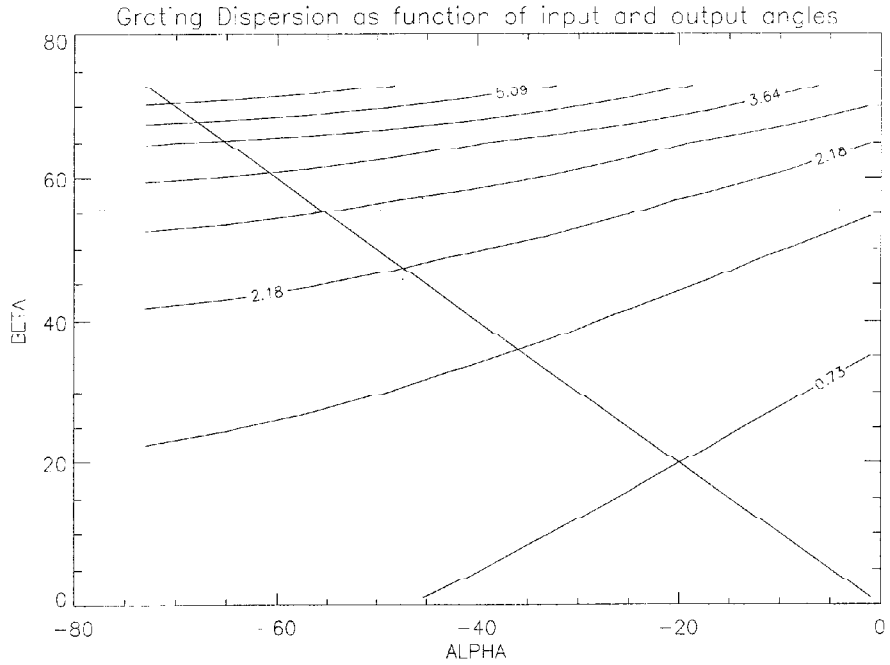

Figure 1

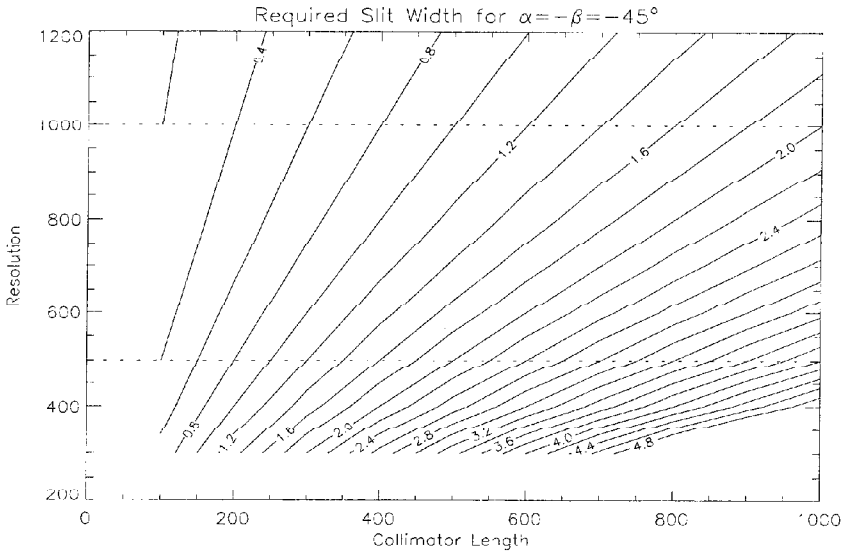

Figure 2

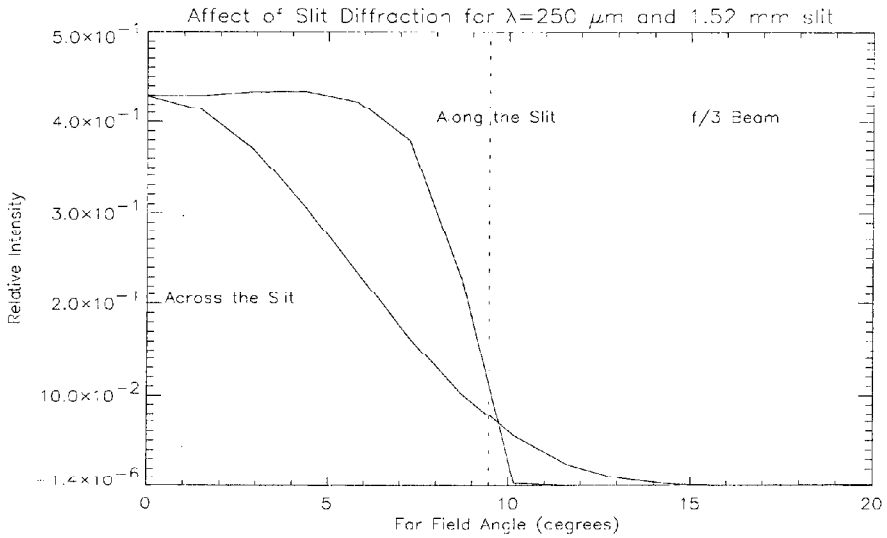

Figure 3

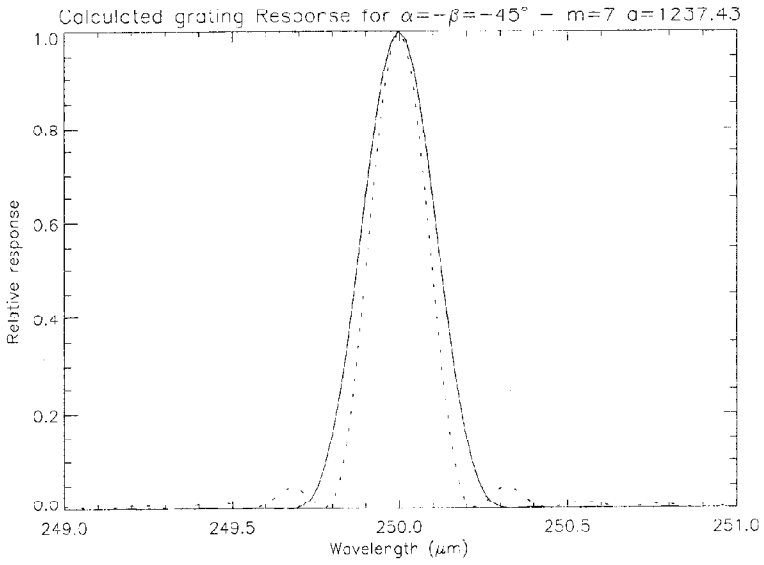

Figure 4

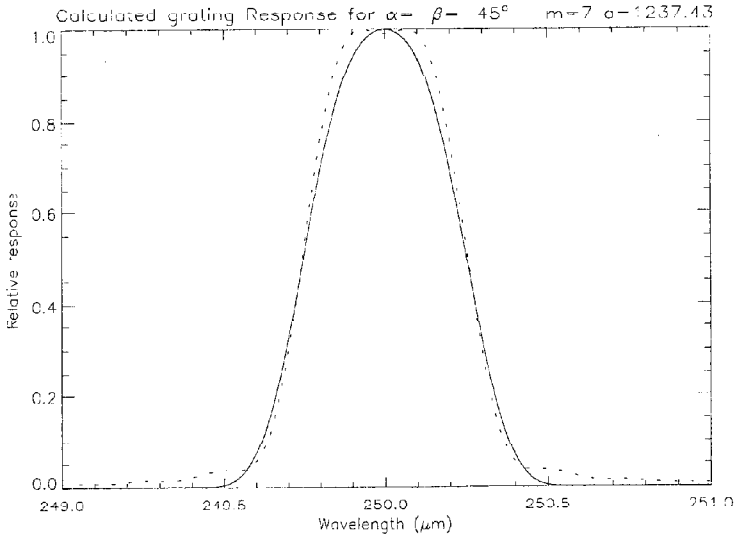

Figure 5

CROSS DISPERSING.

ECHELLE $\alpha = -45°$

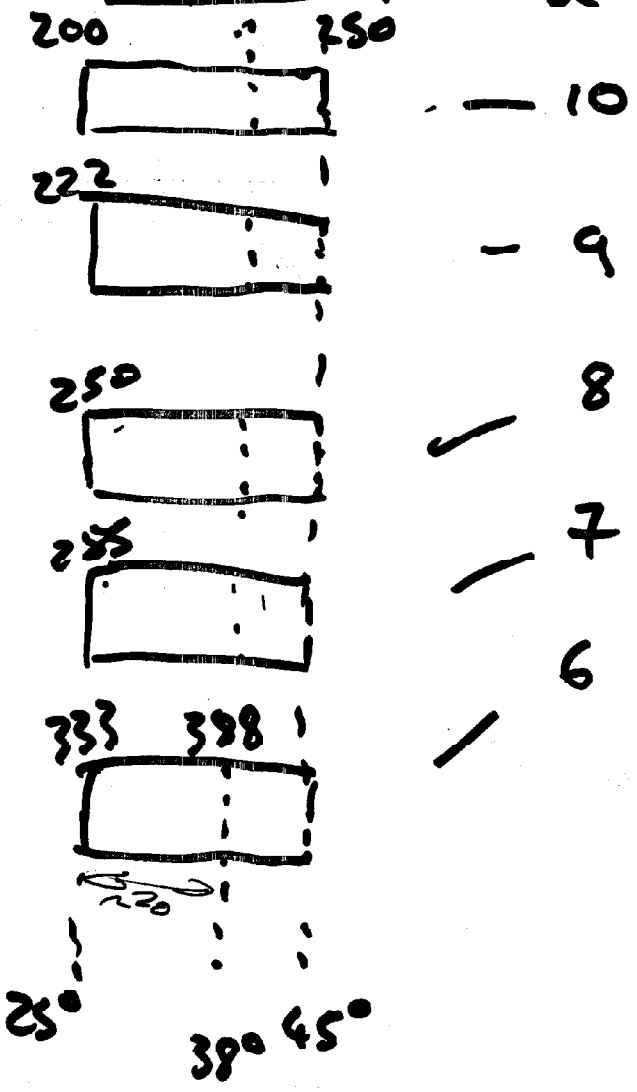

⇒ 1 Pixel ≡ $\Delta\lambda$

⇒ Have to scan only $\pm \frac{\Delta\lambda}{4}$

MULTIPLEX ≥ 20

IID DEFINITION

- QUICK UPDATE NEXT WEEK [MJG + BM + ?]
- DETAILED REVISION FOR JUNE 4
  - CRYOHARNESS [MJG + BM]
  - MASSES [PRM ETC.]
  - DATA RATE [KJK ET AL]
  - THERMAL LOADS [CRC]
  - REVISION OF DESCRIPTION ETC. [MJG + BMS]